Report

Current Biology

Two Early Cretaceous Fossils Document Transitional Stages in Alvarezsaurian Dinosaur Evolution

Graphical Abstract

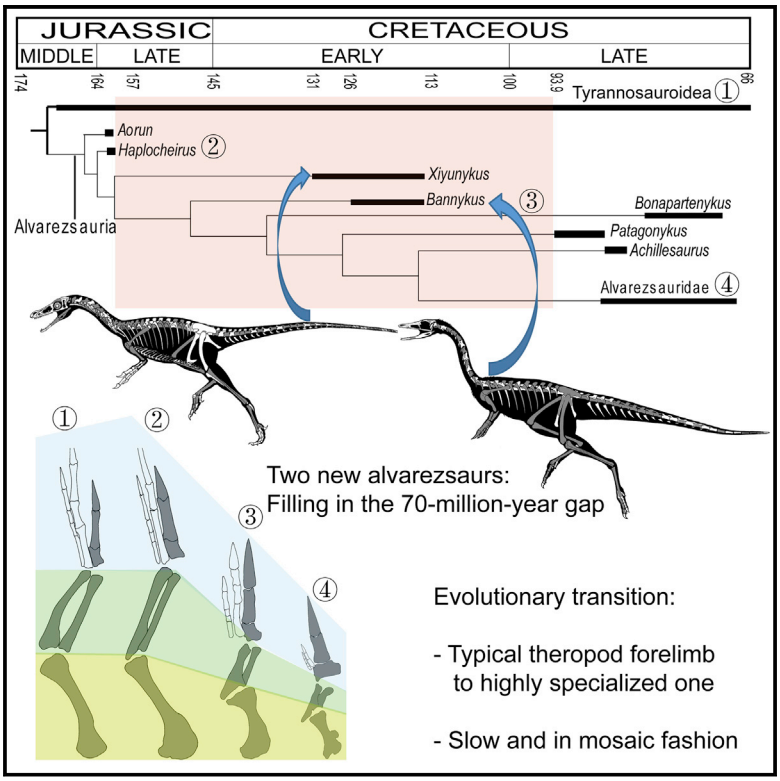

Highlights

- Two new alvarezsaurian dinosaurs are described from Northwest China
- They are intermediate between Late Jurassic and Late Cretaceous alvarezsaurians
- They showcase the evolution of highly specialized alvarezsaurian forelimb
- Specialized alvarezsaurian forelimb morphology evolved slowly, in a mosaic fashion

Authors

Xing Xu, Jonah Choiniere, Qingwei Tan, ..., Shuo Wang, Hai Xing, Lin Tan

Correspondence

xingxu@vip.sina.com

In Brief

Xu et al. report two new Early Cretaceous alvarezsaurian theropods representing transitional stages in alvarezsaurian evolution. The analyses indicate that the evolutionary transition from a typical theropod forelimb configuration to a highly specialized one was slow and occurred in a mosaic fashion during the Cretaceous.

Xu et al., 2018, Current Biology *28*, 1–8
September 10, 2018
https://doi.org/10.1016/j.cub.2018.07.057

CellPress

Please cite this article in press as: Xu et al., Two Early Cretaceous Fossils Document Transitional Stages in Alvarezsaurian Dinosaur Evolution, Current Biology (2018), https://doi.org/10.1016/j.cub.2018.07.057

Current Biology
Report

Two Early Cretaceous Fossils Document Transitional Stages in Alvarezsaurian Dinosaur Evolution

Xing Xu,[1,2,3,16,17,*] Jonah Choiniere,[4,5,16] Qingwei Tan,[6] Roger B.J. Benson,[4,7,16] James Clark,[8,9] Corwin Sullivan,[10,11] Qi Zhao,[1] Fenglu Han,[12] Qingyu Ma,[1] Yiming He,[13] Shuo Wang,[14] Hai Xing,[15] and Lin Tan[6]

[1]Key Laboratory of Vertebrate Evolution and Human Origins, Institute of Vertebrate Paleontology and Paleoanthropology, Chinese Academy of Sciences, 142 Xiwai Street, Beijing 100044, China
[2]CAS Center for Excellence in Life and Paleoenvironment, 142 Xiwai Street, Beijing 100044, China
[3]Centre for Research and Education on Biological Evolution and Environment, 163 Xianlin Road, Nanjing University, Nanjing 210045, China
[4]Evolutionary Studies Institute, University of the Witwatersrand, Private Bag 3, Johannesburg WITS 2050, South Africa
[5]Department of Vertebrate Paleontology and Richard Gilder Graduate School, American Museum of Natural History, Central Park West at 79th Street, New York, NY 10024, USA
[6]Long Hao Institute of Geology and Paleontology, Jia 29, Fengzhou Road, Hohhot, Nei Mongol 010010, China
[7]Department of Earth Sciences, University of Oxford, South Parks Road, Oxford OX1 3AN, UK
[8]Department of Biological Sciences, George Washington University, 2023 G Street NW, Washington, DC 20052, USA
[9]Centre for Vertebrate Evolutionary Biology, Yunnan University, 2 Green Lake North Road, Kunming 650091, China
[10]Department of Biological Sciences, University of Alberta, 11455 Saskatchewan Drive, Edmonton, AB T6G 2E9, Canada
[11]Philip J. Currie Dinosaur Museum, 9301 112 Avenue, Wembley, AB T0H 3S0, Canada
[12]School of Earth Sciences, China University of Geosciences, 388 Lumo Road, Wuhan 430074, China
[13]School of Earth Sciences and Engineering, Nanjing University, 163 Xianlin Road, Nanjing 210045, China
[14]College of Life Science, Capital Normal Univerity, 105 West 3rd Ring Road North, Beijing 100048, China
[15]Beijing Museum of Natural History, Beijing Academy of Science and Technology, 126 South Tianqiao Street, Beijing 100050, China
[16]These authors contributed equally
[17]Lead Contact
*Correspondence: xingxu@vip.sina.com
https://doi.org/10.1016/j.cub.2018.07.057

SUMMARY

Highly specialized animals are often difficult to place phylogenetically. The Late Cretaceous members of Alvarezsauria represent such an example, having been posited as members of various theropod lineages, including birds [1–11]. A 70-million-year ghost lineage exists between them and the Late Jurassic putative alvarezsaurian *Haplocheirus* [12], which preserves so few derived features that its membership in Alvarezsauria has recently been questioned [13]. If *Haplocheirus* is indeed an alvarezsaurian, then the 70-million-year gap between *Haplocheirus* and other alvarezsaurians represents the longest temporal hiatus within the fossil record of any theropod subgroup [14]. Here we report two new alvarezsaurians from the Early Cretaceous of Western China that document successive, transitional stages in alvarezsaurian evolution. They provide further support for *Haplocheirus* as an alvarezsaurian and for alvarezsaurians as basal maniraptorans. Furthermore, they suggest that the early biogeographic history of the Alvarezsauria involved dispersals from Asia to other continents. The new specimens are temporally, morphologically, and functionally intermediate between *Haplocheirus* and other known alvarezsaurians and provide a striking example of the evolutionary transition from a typical theropod forelimb configuration (i.e., the relatively long arm and three-digit grasping hand of typical tetanuran form in early-branching alvarezsaurians) to a highly specialized one (i.e., the highly modified and shortened arm and one-digit digging hand of Late Cretaceous parvicursorines such as *Linhenykus* [1, 15]). Comprehensive analyses incorporating data from these new finds show that the specialized alvarezsaurian forelimb morphology evolved slowly and in a mosaic fashion during the Cretaceous.

RESULTS AND DISCUSSION

Systematic Paleontology

Dinosauria Owen, 1842 [16].
Theropoda Marsh, 1881 [17].
Alvarezsauria Bonaparte, 1991 [2].
Xiyunykus pengi gen. et sp. nov. (Figure 1).

Etymology

"*Xiyu*" (Mandarin), western regions, referring to Central Asia including Xinjiang, and "*onyx*" (Greek), claw; the specific name is in honor of Professor Peng Xiling, who has contributed greatly to the study of geology in Xinjiang.

Holotype

The holotype is a partial, disarticulated skeleton (Figure 1A), cataloged as IVPP (Institute of Vertebrate Paleontology and Paleoanthropology) V22783.

Locality and Horizon

Wucaiwan area, Junggar Basin, Xinjiang, China; Upper Cretaceous (Barremian-Aptian?) upper part of the Tugulu Group [18].

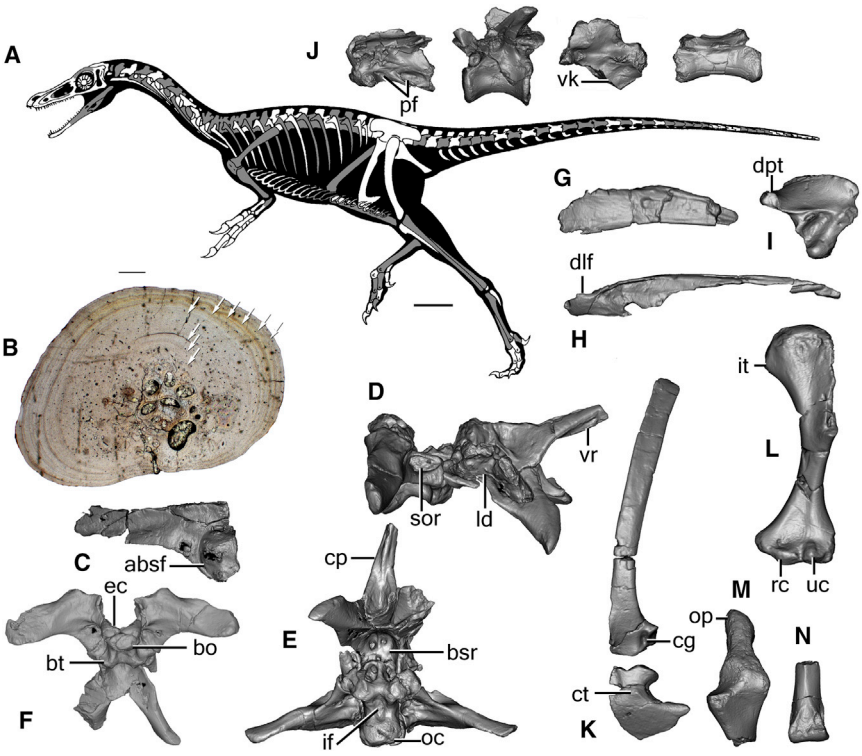

Figure 1. Skeletal Anatomy of *Xiyunykus pengi* IVPP V22783

(A) Skeletal silhouette showing preserved bones (in gray).

(B) Histological thin-section of the fibula. Arrows denote growth lines used to age the specimen (see Data S1 for a detailed explanation).

(C) Left frontal in dorsal view.

(D–F) Partial braincase in left lateral (D), ventral (E), and posterior (F) views.

(G and H) Right dentary (G) and right surangular (H) in lateral view.

(I) Left articular in dorsal view.

(J) Vertebrae in left lateral view, including a middle cervical (left), a middle dorsal (middle left), the last sacral (middle right), and a posterior caudal (right).

(K) Left scapula and coracoid in lateral view.

(L) Left humerus in anterior view.

(M) Right ulna in anterior view.

(N) Partial left metatarsal III in ventral view.

The scale bar represents 100 mm for (A) and 500 μm for (B). Abbreviations: absf, anterior border of supratemporal fossa; bo, basioccipital; bt, basal tuber; bsr, basisphenoid recess; cg, curved groove; cp, cultriform process; ct, coracoid tubercle; dlf, dorsolateral flange; dpt, dorsomedially projecting tab; ec, exoccipital; if, infracondylar fossa; it, internal tuberosity; ld, lateral depression; oc, occipital condyle; op, olecranon process; pf, pneumatic fossa; rc, radial condyle; sor, subotic recess; uc, ulnar condyle; vk ventral keel; vr, ventral ridge. No scale for (C)–(N). See also Table S1.

Diagnosis

Distinguishable from other alvarezsaurians, to the extent that they are known, in possessing the following autapomorphies: large basal tubera formed exclusively by basioccipital; basisphenoid recess with basioccipital contribution and containing multiple deep fossae; cultriform process with poorly ossified dorsal margin that parallels ventral margin in lateral view; two horizontally arranged pneumatic fossae on lateral central surface of each anterior or middle cervical vertebra; distinct tubercle along ventrolateral edge of each anterior cervical centrum; groove present medial to each posterior cervical epipophysis; posterior surface of each cervical and dorsal neural arch bearing multiple deep fossae above neural canal; deep, curved groove on scapular lateral surface immediately anterior to glenoid fossa; long, deep groove along posterior edge of proximal half of scapular blade; sharp and short groove on lateral surface of femoral distal end; and proximal end of tibia with deep groove on posterior condyle.

Description and Comparisons

The holotype of *Xiyunykus pengi* is estimated to have had a body mass of 15 kg, based on femoral shaft circumference [19]. Based on histological analysis, this individual was in its ninth year of life and was probably a sub-adult (Data S1; Figure 1B).

Xiyunykus possesses a cranial morphology (Figures 1C–1I) that is transitional between the early-branching alvarezsaurian *Haplocheirus* and parvicursorine alvarezsaurians [1, 20]. Most preserved elements, including the frontal, opisthotic-exoccipital complex, dentary, angular, and surangular, are nearly identical in general morphology to those of *Haplocheirus*. However, a few cranial features, including a prominent ventral ridge on the cultriform process and a large dorsomedially projecting tab on the retroarticular process of the articular, are reminiscent of specialized parvicursorine alvarezsaurians such as *Shuvuuia* [5]. *Xiyunykus* also homoplastically shares several derived cranial features (Figures 1C–1I) with the early-branching coelurosaurian group Ornithomimosauria [21], including (1) anterior border of supratemporal fossa strongly convex and located on posterolateral corner of frontal; (2) basioccipital excluded from foramen magnum by exoccipitals; (3) ''lateral depression'' present on lateral wall of braincase (also known in troodontids) [21, 22]; (4) infracondylar fossa present ventral to occipital condyle; (5) well-developed subcondylar and subotic recesses; (6) inflated, hollow cultriform process; (7) dentary sub-triangular in lateral view; and (8) surangular with dorsolateral flange lateral to glenoid region. Features 2, 3, 4, and 6 are absent in *Haplocheirus*, and whether feature 5 is also absent cannot be ascertained.

Similar to alvarezsaurids, all cervical centra are strongly opisthocoelous, the anterior dorsal centra are weakly opisthocoelous, and the last sacral centrum possesses a large ventral keel (Figure 1J). In contrast, each preserved caudal centrum is plesiomorphically amphicoelous (Figure 1J) and lacks a deep ventral sulcus. The scapula is proportionally long, rather than short as in parvicursorines [1], and the coracoid has a pyramidal but very small coracoid tubercle (Figure 1K). The humerus is plesiomorphic in being relatively slender, having a relatively small and distally located internal tuberosity, and bearing distally projecting radial and ulnar condyles (Figure 1L), but the ulna shows incipiently developed derived features including a proximally projecting, laterally compressed olecranon process (Figure 1M). The hind limbs largely show a plesiomorphic coelurosaurian

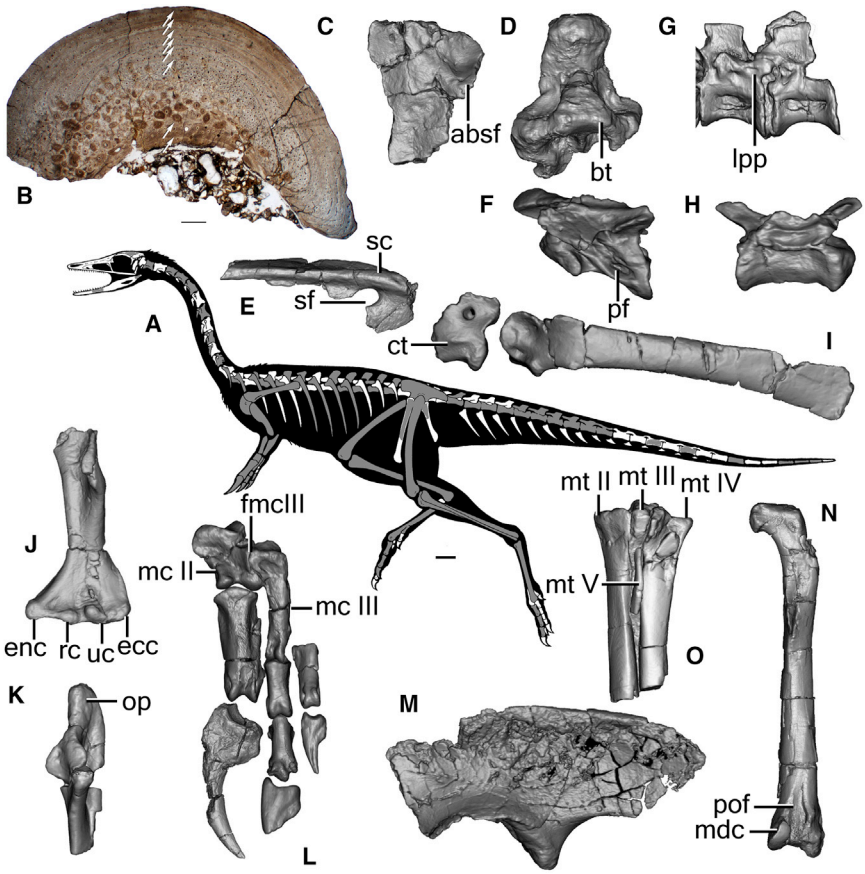

Figure 2. Skeletal Anatomy of *Bannykus wulatensis* IVPP V25026

(A) Skeletal silhouette showing preserved bones (in gray).
(B) Histological thin-section of the fibula.
(C) Left frontal in dorsal view.
(D) Basioccipital in ventral view.
(E) Left surangular in lateral view.
(F–H) Vertebrae in left lateral view, including a middle cervical (F), a middle dorsal (G), and a middle caudal (H).
(I) Left scapula and coracoid in lateral view.
(J and K) Left humerus (J) and left ulna (K) in anterior view.
(L) Left manus in anterior view.
(M) Left ilium in lateral view.
(N) Right femur in posterior view.
(O) Right metatarsals in posterior view.
The scale bar represents 100 mm for (A) and 500 μm for (B). Abbreviations: absf, anterior border of supratemporal fossa; bt, basal tuber; ct, coracoid tubercle; ecc, ectepicondyle; enc, entepicondyle; fmcIII, facet for metacarpal III; lpp, laterally protruding parapophysis; mc II-III, metacarpals II-III; mdc, medial distal condyle; mt II-V. metatarsals II-V; pof, popliteal fossa; oc, occipital condyle; op, olecranon process; pf, pneumatic fossa; rc, radial condyle; uc, ulnar condyle; sc, surangular crest; sf, surangular foramen. See also Table S1.

morphology, but also display several features seen in parvicursorines. For example, the distal portion of the shaft of metatarsal III is sub-triangular in cross section (Figure 1N).

Dinosauria Owen, 1842 [16].

Theropoda Marsh, 1881 [17].

Alvarezsauria Bonaparte, 1991 [2].

Bannykus wulatensis gen. et sp. nov. (Figure 2).

Etymology

"*Ban*" (Mandarin), half, referring to the transitional features seen in this animal, and "*onyx*" (Greek), claw; the specific name is derived from Wulatehouqi (Wulate Rear Banner), the county-level administrative division in which the type locality is situated.

Holotype

The holotype specimen is a partial, semi-articulated skeleton (Figure 2A), cataloged as IVPP V25026.

Locality and Horizon

Chaoge, Wulatehouqi, Inner Mongolia, China; Lower Cretaceous (Aptian) Bayingobi Formation [23].

Diagnosis

Differs from other alvarezsaurians in possessing the following autapomorphies: notch between basal tubera nearly absent; surangular foramen large; posterior dorsal vertebrae with distal ends of transverse processes strongly expanded in posterior direction; humeral internal tuberosity deflected posteriorly; well-developed facet on lateral surface of metacarpal II for articulation with metacarpal III; metacarpal III curved medially; prominent ventral heel at proximal end of manual phalanx III-1; manual phalanx III-2 with proximoventrally located tubercles on medial and lateral surfaces and two sulci bounded by three parallel condyles on distal end; manual phalanx III-3 without median vertical ridge on proximal articular surface (note that we identify the three manual digits of tetanurans as II-III-IV following some recent paleontological studies [24]); posterolateral margin of fibular condyle of tibia bears pyramidal lateral projection; and deep groove along posterior margin of proximal half of fibular crest.

Description and Comparisons

The holotype individual of *Bannykus wulatensis* is estimated to have had a body mass of 24 kg, based on femoral circumference [19]. Based on histological analysis, it was in its eighth year of life and was probably a sub-adult (Data S1; Figure 2B).

Bannykus is more similar in its preserved cranial morphology to parvicursorines such as *Shuvuuia* than to *Xiyunykus* and *Haplocheirus*. For example, the supratemporal fossa is poorly defined anteriorly, the infracondylar fossa is absent, and the surangular crest is relatively indistinct (Figures 2C–2E).

Bannykus possesses many of the vertebral features described above for *Xiyunykus*, but it also shares some additional derived features with early-branching alvarezsaurids and even parvicursorines (Figures 2F–2H): the cervical centra each have a ventral groove, the dorsal vertebrae have laterally protruding parapophyses, the anteriormost caudal centra are ventrally keeled, and most of the caudal vertebrae are procoelous and bear deep sulci on their ventral surfaces. *Bannykus* is also transitional between *Xiyunykus* and Late Cretaceous alvarezsaurians in the morphology of the scapula and coracoid [1]: the scapular blade is nearly straight and the coracoid bears a weak, ridge-like coracoid tubercle (Figure 2I).

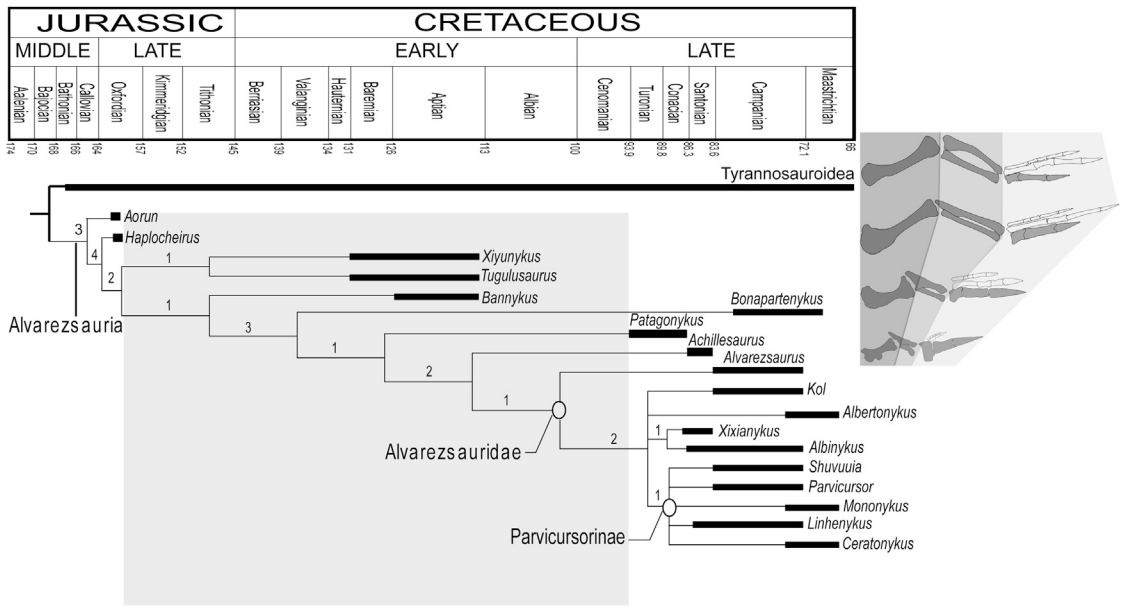

Figure 3. Time-Calibrated Simplified Theropod Phylogeny Showing Evolution of Alvarezsaurian Forelimb

Forelimbs scaled to the femoral length of the generalized basal coelurosaur *Guanlong* (top) and selected alvarezsaurians. Note the medial finger (in gray) enlargement and lateral finger reduction in *Haplocheirus* (upper middle), significant forelimb shortening and further forelimb modification in *Bannykus* (lower middle), and extremely shortened and specialized forelimb in *Shuvuuia* (bottom). Numbers above nodes indicate Bremer Support values when *Kol ghuva* is excluded from support calculation. The gray rectangle indicates the temporal span of the previous gap in the alvarezsaurian fossil record. See also Figures S1 and S2.

The forelimbs of *Bannykus* are highly modified, but not to the degree seen in Late Cretaceous alvarezsaurians [1, 25]. The humerus is 38% as long as the femur and has a similar mid-shaft diameter. The humerus bears a large, proximally projecting, trapezoidal internal tuberosity, as well as a large and distally located ectepicondyle and entepicondyle [12], but it is plesiomorphic in that the internal tuberosity, ectepicondyle, and entepicondyle are not hypertrophied, sub-spherical structures (Figure 2J). The ulna has a mediolaterally compressed olecranon process (Figure 2K) that is intermediate in size between those of *Xiyunykus* and Late Cretaceous alvarezsaurians [1, 12]. Manual digit II is significantly enlarged, and digit IV is shortened (Figure 2L), but neither is modified to the degree seen in alvarezsaurids [15, 25, 26]. Metacarpal II bears a deep notch on its lateral surface for articulation with metacarpal III (Figure 2L), whereas these two metacarpals are tightly syndesmosed or co-ossified in alvarezsaurids [1].

The ilium is plesiomorphic in lacking all modifications (Figure 2M) seen in Late Cretaceous alvarezsaurians [1]. The hind limbs are generally similar to those of *X. pengi*, but they display a few apomorphic features. The medial distal condyle of the femur is transversely flattened, and the popliteal fossa is bounded laterally and medially by two ridges (Figure 2N). The distal end of the tibia has only two facets for articulation with the proximal tarsals, and the proximal end of metatarsal III is strongly compressed (Figure 2O).

Phylogenetic Analysis

Until now, there have been no transitional alvarezsaurians linking the plesiomorphic morphology of the Late Jurassic *Haplocheirus* [12] to the more derived anatomical features of Upper Cretaceous alvarezsaurians [2, 15, 27–29]. This lack of evidence was manifest in a recent maximum-likelihood analysis that suggested that *Haplocheirus* was instead an early-branching ornithomimosaur, whereas the Late Cretaceous alvarezsaurians constituted a clade within Avialae [13]. The relatively large Early Cretaceous alvarezsaurians (Table S1) *Xiyunykus* and *Bannykus* interrupt the long branch leading to Late Cretaceous members of the clade and provide clear morphological evidence linking these advanced taxa to *Haplocheirus*. Our phylogenetic analysis places *Xiyunykus* and *Bannykus* successively closer to the short-armed, Late Cretaceous alvarezsaurians, confirms a relatively basal position for Alvarezsauria within Maniraptora, and places *Haplocheirus* firmly within Alvarezsauria (Data S1). Somewhat surprisingly, it also groups the Late Jurassic Shishugou form *Aorun* [20] and the enigmatic Early Cretaceous Tugulu Formation theropod *Tugulusaurus* [30] within Alvarezsauria, suggesting that early-branching alvarezsaurians were more common than previously thought (Figures 3 and S1).

Alvarezsaurian Biogeography

The phylogenetic positions of the Late Jurassic *Aorun* and *Haplocheirus* and the Early Cretaceous *Xiyunykus*, *Tugulusaurus*, and *Bannykus* along the stem of Alvarezsauria suggest that dispersal [15, 27, 31, 32], rather than vicariance (e.g., [28, 33]), characterizes the early biogeographic history of the group, given that all of these taxa are Asian. More specifically, our analysis indicates that alvarezsaurians originated in Asia and remained there throughout the Cretaceous, with dispersal to other continents occurring after the appearance of *Bannykus* and

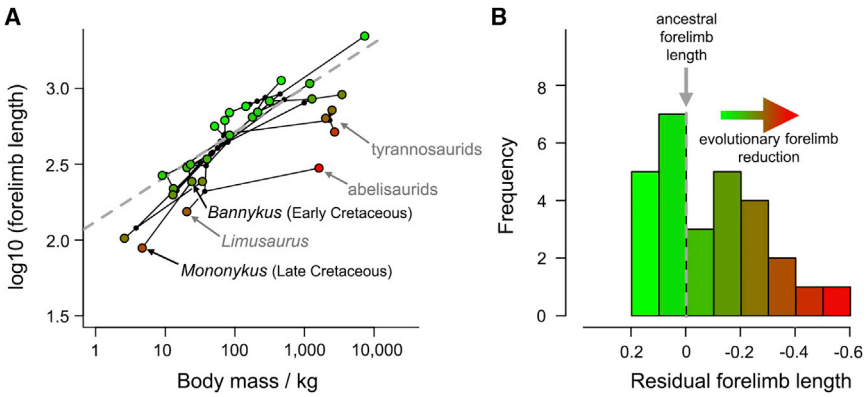

Figure 4. Relationship of Forelimb Length with Body Mass in Non-paravian Theropods and Reduction of the Alvarezsaurian Forelimb

(A) Phylomorphospace showing relationship of partial forelimb length with body mass, with points colored according to residuals from the phylogenetic generalized least-squares regression (dashed, gray line; $\log_{10}$(arm length) = 0.30 × $\log_{10}$(body mass + 2.12, $p < 0.001$, N = 28; Table S2)).

(B) Histogram of residuals from the regression in (A) showing the extent of forelimb reduction in alvarezsaurians and that theropods in general underwent greater proportional forelimb reduction than enlargement compared to their ancestor (ancestor residual = 0.0).

See also Figure S3.

Xiyunykus. The alternative vicariance hypothesis would involve alvarezsaurians spreading throughout Pangaea before the Aptian, with different species ending up on different continents as Pangaea broke apart. The dispersal hypothesis is also supported by our statistical biogeographical analysis (Data S1; Figure S2). Previous studies have suggested a vicariant distribution of several theropod lineages including alvarezsaurids based on either the relatively basal positions or the endemic nature of Gondwanan taxa within their respective clades [34]. Our results illustrate the potential of increased taxon sampling to change biogeographic inferences.

Mosaic Evolution

As phylogenetically, temporally, and morphologically transitional forms, the two new alvarezsaurians illuminate the pattern, pace, and timing of evolution of the bizarre, highly specialized alvarezsaurian skeleton [35], and particularly the forelimb (Figure 3). Our analysis shows that alvarezsaurian skeletal evolution occurred in a somewhat modular manner, with different skeletal parts being modified at different evolutionary rates. The presacral and sacral vertebrae were evidently modified earlier than the caudal vertebrae, and the pectoral girdle and forelimb earlier than the pelvic girdle and hindlimb, implying a general pattern in which anterior parts of the skeleton were modified earlier than posterior parts. To some degree the tail, pelvis, and hindlimbs acted as an integrated locomotor unit in non-avian dinosaurs because of the role of the caudofemoralis muscle in femoral retraction [36], and patterns of alvarezsaurian skeletal evolution suggest that this locomotor unit might have been relatively conservative in evolutionary terms.

Forelimb Reduction and Modification

Phylogenetic regression provides strong evidence for weak negative allometry of forelimb length in non-paravian theropods (Data S1; Table S2). *Bannykus* shows slight proportional reduction of the forelimb compared to *Haplocheirus*, and the same was true of *Xiyunykus*, based on the similar sizes of the preserved elements. Nevertheless, the forelimbs of these Early Cretaceous alvarezsaurians were relatively unreduced compared to those of other theropods (Figures 4 and S3) and therefore unlike those of Late Cretaceous alvarezsaurians (parvicursorines, represented by *Mononykus*). Parvicursorines display a level of proportional arm reduction that is among the greatest seen in any dinosaur group, being exceeded only in some tyrannosaurids and abelisaurids (Figure 4A). Our results show that this extreme arm reduction occurred late in alvarezsaurian evolution, and at small body mass (estimated around 24 kg; Figure 4A).

The new finds demonstrate that some key functional features of the parvicursorine forelimb were also present in Early Cretaceous alvarezsaurians. These include increased olecranon length and digit robustness, which respectively increased the extensor moment arm of the elbow joint and the mechanical strength of the hand. These features may suggest that the forelimb had a fossorial function in the Early Cretaceous taxa, as well as in parvicursorines [27, 37]. Nevertheless, other characteristic parvicursorine features, including substantial forelimb length reduction, are absent in our Early Cretaceous specimens, showing that the extreme forelimb modifications seen in Late Cretaceous alvarezsaurians evolved incrementally (Figure 3). This is best exemplified by the manus, which in parvicursorines is the most obviously specialized body part. The Late Jurassic *Haplocheirus* has a grasping hand as in typical theropods, though it shows several alvarezsaurid features in an incipient form [12]. The Early Cretaceous *Bannykus*, by contrast, possesses a dorsoventrally compressed hand with a hypertrophied thumb and shortened lateral digits (though some unusual manual features in *Bannykus* suggest a specialized function; see Data S1), indicating a shift away from grasping function. Finally, the Late Cretaceous alvarezsaurians have a highly specialized hand with only one functional digit, namely, a thumb that is even more enlarged than in *Bannykus* (best exemplified by the monodactyl *Linhenykus* [15]). The highly reduced length of the parvicursorine forelimb has been a source of functional controversy [3, 27, 28, 37, 38], with some research suggesting that it would not have been long enough to function effectively in fossorial activities [27, 28, 39]. *Bannykus* and *Xiyunykus* share many of the fossorial features of the forelimb of parvicursorines but retain a plesiomorphically longer forelimb. Thus, early modification of the alvarezsaurian forelimb would have no conflict with fossorial function, and perhaps only the most derived parvicursorine forelimbs were used in a different fashion. Alvarezsaurian digit reduction occurred over 50 million years, about half the total duration of alvarezsaurian evolution (~95 million years). This provides a striking example of digit reduction and specialization

among theropods, comparable to the classic example in horse evolution [40].

STAR★METHODS

Detailed methods are provided in the online version of this paper and include the following:

- KEY RESOURCES TABLE
- CONTACT FOR REAGENT AND RESOURCE SHARING
- EXPERIMENTAL MODEL AND SUBJECT DETAILS
- METHOD DETAILS
  - CT images
  - Histology
  - Phylogenetic analysis
  - Biogeographic inference
  - Analysis of forelimb allometry and reduction
- DATA AND SOFTWARE AVAILABILITY
  - Nomenclature

SUPPLEMENTAL INFORMATION

Supplemental Information includes three figures, two tables, and one data file and can be found with this article online at https://doi.org/10.1016/j.cub.2018.07.057.

ACKNOWLEDGMENTS

We thank Gao Hong, Bayaer, Zhiqiang Bao, Jianmin Wang, Jinsheng Liu, and Dong Xiao for coordinating the fieldwork in Inner Mongolia, as well as Hongjun Chu and Dengjie Ma for doing the same in Xinjiang. We also thank Tao Yu for discovering IVPP V22783, Jianqiang Hao for discovering IVPP V25026, Haijun Wang and Jianqiang Hao for collecting the specimens, Rongshan Li for the line drawings, Yun Feng for computed tomography images, and Lishi Xiang, Tao Yu, and Xiaoqing Ding for preparing the specimens. This work is supported by the National Natural Science Foundation of China (grant nos. 41688103, 91514302, 41120124002, 41602013, and 41602006), the Strategic Priority Research Program of the Chinese Academy of Sciences (grant no. XDB18030504), and the US NSF (EAR 0922187). J.N.C. was supported by the DST (AOP #98800) and NRF (IRG #95449) of South Africa, by the Palaeontological Scientific Trust (PAST), by the Kalbfleisch and Gerstner Scholarship of the Richard Gilder Graduate School, American Museum of Natural History, and by the Friedel Sellschop Award. R.B.J.B. was supported by the European Union's Horizon 2020 Research and Innovation program 2014–2018 under grant agreement 677774 (ERC Starting Grant: TEMPO). H.X. was supported by the Beijing Academy of Science and Technology Innovative Team Program (IG201705N).

AUTHOR CONTRIBUTIONS

X.X., J.C., J.N.C., and R.B.J.B. designed the research project. J.N.C. conducted the phylogenetic analysis, R.B.J.B. the forelimb reduction analysis, Q.Z. the histological analysis, and H.X. the biogeographical analysis. X.X., J.N.C., Q.T., J.C., C.S., Q.Z., F.H., Q.M., Y.H., S.W., H.X., and L.T. collected and analyzed the specimens. X.X., J.N.C., R.B.J.B., J.C., Q.Z., H.X., and C.S. wrote the manuscript.

DECLARATION OF INTERESTS

The authors declare no competing interests.

Received: April 23, 2018
Revised: June 4, 2018
Accepted: July 24, 2018
Published: August 23, 2018

REFERENCES

1. Chiappe, L.M., Norell, M.A., and Clark, J.M. (2002). The Cretaceous, short-armed Alvarezsauridae: *Mononykus* and its kin. In Mesozoic Birds: Above the Heads of Dinosaurs, L.M. Chiappe, and L.M. Witmer, eds. (University of California Press), pp. 87–120.
2. Bonaparte, J.F. (1991). Los vertebrados fósiles de la Formación Río Colorado, de la ciudad de Neuquén y cercanías, Cretácico superior, Argentina. Rev. del Museo argent. de Ciencias Naturales" Bernardino Rivadavia. Paleontologia *4*, 17–123.
3. Perle, A., Norell, M.A., Chiappe, L., and Clark, J.M. (1993). Flightless bird from the Cretaceous of Mongolia. Nature *362*, 623–626.
4. Naish, D., and Dyke, G.J. (2004). *Heptasteornis* was no ornithomimid, troodontid, dromaeosaurid or owl: the first alvarezsaurid (Dinosauria: Theropoda) from Europe. Neues Jahrb. Geol. Palaontol., Monatsh. *7*, 385–401.
5. Chiappe, L.M., Norell, M.A., and Clark, J.M. (1998). The skull of a relative of the stem-group bird *Mononykus*. Nature *392*, 275–278.
6. Sereno, P.C. (1999). Dinosaurian biogeography; vicariance, dispersal and regional extinction. National Science Museum Monographs *15*, 249–257.
7. Rauhut, O.W.M. (2003). The interrelationships and evolution of basal theropod dinosaurs. Palaeontology *69*, 1–215.
8. Norell, M.A., Clark, J.M., and Makovicky, P.J. (2001). Phylogenetic relationships among coelurosaurian dinosaurs. In New Perspectives on the Origin and Evolution of Birds, J. Gauthier, and L.F. Gall, eds. (Yale University Press), pp. 49–67.
9. Turner, A.H., Pol, D., Clarke, J.A., Erickson, G.M., and Norell, M.A. (2007). A basal dromaeosaurid and size evolution preceding avian flight. Science *317*, 1378–1381.
10. Senter, P. (2007). A new look at the phylogeny of coelurosauria (Dlnosauria: Theropoda). J. Syst. Palaeontology *5*, 429–463.
11. Holtz, T., and Jr, R. (1998). A new phylogeny of the carnivorous dinosaurs. Gaia *15*, 5–61.
12. Choiniere, J.N., Xu, X., Clark, J.M., Forster, C.A., Guo, Y., and Han, F. (2010). A basal alvarezsauroid theropod from the early Late Jurassic of Xinjiang, China. Science *327*, 571–574.
13. Lee, M.S.Y., and Worthy, T.H. (2012). Likelihood reinstates *Archaeopteryx* as a primitive bird. Biol. Lett. *8*, 299–303.
14. Weishampel, D.B., Barrett, P.M., Coria, R.A., Loeuff, J.L., Xu, X., Zhao, X.J., Sahni, A., Gomani, E., and Noto, C.R. (2004). Dinosaur distribution. In The Dinosauria, Second Edition, D.B. Weishampel, P. Dodson, and H. Osmolska, eds. (University of California Press), pp. 517–606.
15. Xu, X., Sullivan, C., Pittman, M., Choiniere, J.N., Hone, D., Upchurch, P., Tan, Q., Xiao, D., Tan, L., and Han, F. (2011). A monodactyl nonavian dinosaur and the complex evolution of the alvarezsauroid hand. Proc. Natl. Acad. Sci. USA *108*, 2338–2342.
16. Owen, R. (1842). Report on british fossil reptiles. Part II. Report of the British Association for the Advancement of Science *11*, 60–204.
17. Marsh, O.C. (1881). Classification of the Dinosauria. American Journal of Science *18* (Series 3), 81–86.
18. Eberth, D.A., Brinkman, D.B., Chen, P.-J., Yuan, F.-T., Wu, S.-Z., Li, G., and Cheng, X.-S. (2001). Sequence stratigraphy, paleoclimate patterns, and vertebrate fossil preservation in Jurassic Cretaceous strata of the Junggar Basin, Xinjiang Autonomous Region, People's Republic of China. Can. J. Earth Sci. *38*, 1627–1644.
19. Campione, N.E., Evans, D.C., Brown, C.M., and Carrano, M.T. (2014). Body mass estimation in non-avian bipeds using a theoretical conversion to quadrupedal stylopodial proportions. Methods Ecol. Evol. *5*, 913–923.
20. Choiniere, J.N., Clark, J.M., Forster, C.A., Norell, M.A., Eberth, D.A., Erickson, G.M., Chu, H., and Xu, X. (2014). A juvenile specimen of a new coelurosaur (Dinosauria: Theropoda) from the Middle–Late Jurassic Shishugou Formation of Xinjiang, People's Republic of China. J. Syst. Palaeontology *12*, 177–215.

21. Makovicky, P.J., Kobayashi, Y., and Currie, P.J. (2004). Ornithomimosauria. In The Dinosauria, Second Edition, D.B. Weishampel, P. Dodson, and H. Osmolska, eds. (University of California Press), pp. 137–150.
22. Makovicky, P.J., Norell, M.A., Clark, J.M., and Rowe, T. (2003). Osteology and relationships of *Byronosaurus jaffei* (Theropda: Troodontidae). Am. Mus. Novit. *3402*, 1–32.
23. Fu, G.B., Li, G.L., Ren, Y.G., Ren, Z.Y., and Ding, L.T. (2007). Early Cretaceous conchostracans from the Bayingebi Formation of Inner Mongolia, China. Acta Palaeontologica Sin. *46*, 244–248.
24. Xu, X., Clark, J.M., Mo, J., Choiniere, J., Forster, C.A., Erickson, G.M., Hone, D.W., Sullivan, C., Eberth, D.A., Nesbitt, S., et al. (2009). A Jurassic ceratosaur from China helps clarify avian digital homologies. Nature *459*, 940–944.
25. Novas, F.E. (1997). Anatomy of *Patagonykus puertai* (Theropoda, Avialae, Alvarezsauridae), from the Late Cretaceous of Patagonia. J. Vertebr. Paleontol. *17*, 137–166.
26. Suzuki, S., Chiappe, L.M., Dyke, G.J., Watabe, M., Barsbold, R., and Tsogtbaatar, K. (2002). A new specimen of *Shuvuuia deserti* Chiappe et al., 1998, from the Mongolian Late Cretaceous with a discussion of the relationships of alvarezsaurids to other theropod dinosaurs (Natural History Museum of Los Angeles County), pp. 1–18.
27. Longrich, N.R., and Currie, P.J. (2009). *Albertonykus borealis*, a new alvarezsaur (Dinosauria: Theropoda) from the Early Maastrichtian of Alberta, Canada: implications for the systematics and ecology of the Alvarezsauridae. Cretac. Res. *30*, 239–252.
28. Novas, F.E. (1996). Alvarezsauridae, Cretaceous maniraptorans from Patagonia and Mongolia. Mem. Queensl. Mus. *39*, 675–702.
29. Sues, H.-D., and Averianov, A. (2016). Ornithomimidae (Dinosauria: Theropoda) from the Bissekty Formation (Upper Cretaceous: Turonian) of Uzbekistan. Cretac. Res. *57*, 90–110.
30. Rauhut, O.W.M., and Xu, X. (2005). The small theropod dinosaurs *Tugulusaurus* and *Phaedrolosaurus* from the Early Cretaceous of Xinjiang, China. J. Vertebr. Paleontol. *25*, 107–118.
31. Averianov, A., and Sues, H.-D. (2017). The oldest record of Alvarezsauridae (Dinosauria: Theropoda) in the Northern Hemisphere. PLoS ONE *12*, e0186254.
32. Martinelli, A.G., and Vera, E. (2007). *Achillesaurus manazzonei*, a new alvarezsaurid theropod (Dinosauria) from the Late Cretaceous Bajo de la Carpa Formation, Río Negro Province, Argentina. Zootaxa *1582*, 1–17.
33. Choiniere, J.N., Forster, C.A., and de Klerk, W.J. (2012). New information on *Nqwebasaurus thwazi*, a coelurosaurian theropod from the Early Cretaceous Kirkwood Formation in South Africa. J. Afr. Earth Sci. *71-72*, 1–17.
34. Makovicky, P.J., Apesteguía, S., and Agnolín, F.L. (2005). The earliest dromaeosaurid theropod from South America. Nature *437*, 1007–1011.
35. Prieto-Márquez, A., Stubbs, T.L., Benton, M.J., and Brusatte, S. (2016). Regional morphological disparity and rates of evolution in coelurosaurian theropod dinosaurs. Journal of Vertebrate Paleontology *36 (Supplement to 5)*, 208.
36. Gatesy, S.M. (1990). Caudofemoral musculature and the evolution of theropod locomotion. Paleobiology *16*, 170–186.
37. Senter, P. (2005). Function in the stunted forelimbs of *Mononykus olecranus* (Theropoda), a dinosaurian anteater. Paleobiology *31*, 373–381.
38. Zhou, Z.H. (1995). Is *Mononykus* a bird? Auk *112*, 958–963.
39. Altangarel, P., Chiappe, L.M., Rinchen, B., Clark, J.M., and Norell, M.A. (1994). Skeletal morphology of *Mononykus olecranus* (Theropoda: Avialae) from the Late Cretaceous of Mongolia. Am. Mus. Novit. *3105*, 1–29.
40. Macfadden, B.J. (2005). Evolution. Fossil horses–evidence for evolution. Science *307*, 1728–1730.
41. Kobayashi, Y., and Barsbold, R. (2005). Reexamination of a primitive ornithomimosaur,*Garudimimus brevipes* Barsbold, 1981 (Dinosauria: Theropoda), from the Late Cretaceous of Mongolia. Can. J. Earth Sci. *42*, 1501–1521.
42. Barsbold, R. (1988). A new Late Cretaceous ornithomimid from the Mongolian People's Republic. Paleontol. J. *22*, 124–127.
43. Maddison, W.P., and Maddison, D.R. (2011). Mesquite: a modular system for evolutionary analysis. Version 2.75. http://www.mesquiteproject.org.
44. Norell, M.A., Clark, J.M., Turner, A., Makovicky, P.J., Barsbold, R., and Rowe, T. (2006). A new dromaeosaurid theropod from Ukhaa Tolgod (Omnogov, Mongolia). Am. Mus. Novit. *3545*, 1–51.
45. Turner, A.H., Makovicky, P.J., and Norell, M.A. (2012). A review of dromaeosaurid systematics and paravian phylogeny. Bull. Am. Mus. Nat. Hist. *371*, 1–206.
46. Zanno, L.E. (2010). A taxonomic and phylogenetic re-evaluation of Therizinosauria (Dinosauria: Maniraptora). J. Syst. Palaeontology *8*, 503–543.
47. Zanno, L.E., and Makovicky, P.J. (2011). Herbivorous ecomorphology and specialization patterns in theropod dinosaur evolution. Proc. Natl. Acad. Sci. USA *108*, 232–237.
48. Agnolin, F.L., Powell, J.E., Novas, F.E., and Kundrat, M. (2012). New alvarezsaurid (Dinosauria, Theropoda) from uppermost Cretaceous of northwestern Patagonia with associated eggs. Cretac. Res. *35*, 33–56.
49. Nesbitt, S.J., Clarke, J.A., Turner, A.H., and Norell, M.A. (2011). A small alvarezsaurid from the eastern Gobi Desert offers insight into evolutionary patterns in the Alvarezsauroidea. J. Vertebr. Paleontol. *31*, 144–153.
50. Goloboff, P.A., Farris, J.S., and Nixon, K.C. (2008). TNT, a free program for phylogenetic analysis. Cladistics *24*, 774–786.
51. Goloboff, P.A. (1999). Analyzing large datasets in reasonable times: solutions for composite optima. Cladistics *15*, 415–428.
52. Goloboff, P.A., Farris, J.S., Källersjö, M., Oxelman, B., Ramírez, M., and Szumik, C.A. (2003). Improvements to resampling measures of group support. Cladistics *19*, 324–332.
53. Bremer, K. (1994). Branch support and tree stability. Cladistics *10*, 295–304.
54. Bremer, K. (1988). The limits of amino acid sequence data in angiosperm phylogenetic reconstruction. Evolution *42*, 795–803.
55. Turner, A.H., Nesbitt, S.J., and Norell, M.A. (2009). A large alvarezsaurid from the Late Cretaceous of Mongolia. Am. Mus. Novit. *3648*, 1–14.
56. The Inkscape Team (2014). Inkscape. https://www.inkscape.org/.
57. Benson, R.B.J., and Choiniere, J.N. (2013). Rates of dinosaur limb evolution provide evidence for exceptional radiation in Mesozoic birds. Proc. Biol. Sci. *280*, 20131780.
58. Benson, R.B.J., Hunt, G., Carrano, M.T., and Campione, N. (2018). Cope's rule and the adaptive landscape of dinosaur body size evolution. Palaeontology *61*, 13–48.
59. Campione, N.E., and Evans, D.C. (2012). A universal scaling relationship between body mass and proximal limb bone dimensions in quadrupedal terrestrial tetrapods. BMC Biol. *10*, 60.
60. Carrano, M.T. (2006). Body-size evolution in the Dinosauria. In Amniote Paleobiology: Perspectives on the Evolution of Mammals, Birds, and Reptiles, M.T. Carrano, T.J. Gaudin, R.W. Blob, and J.R. Wible, eds. (The University of Chicago Press), pp. 225–269.
61. Puttick, M.N., Thomas, G.H., and Benton, M.J. (2014). High rates of evolution preceded the origin of birds. Evolution *68*, 1497–1510.
62. Lee, M.S.Y., Cau, A., Naish, D., and Dyke, G.J. (2014). Dinosaur evolution. Sustained miniaturization and anatomical innovation in the dinosaurian ancestors of birds. Science *345*, 562–566.
63. Dececchi, T.A., and Larsson, H.C. (2013). Body and limb size dissociation at the origin of birds: uncoupling allometric constraints across a macroevolutionary transition. Evolution *67*, 2741–2752.
64. Galton, P.M., and Jensen, J.A. (1979). A new large theropod dinosaur from the Upper Jurassic of Colorado. Brigham Young University Geological Study *26*, 1–12.
65. Siegwarth, J.D., Lindbeck, R.A., Redman, P.D., Southwell, E.H., and Bakker, R.T. (1997). Giant carnivorous dinosaurs of the family Megalosauridae from

the Late Jurassic Morrison Formation of eastern Wyoming. Contributions from the TateMuseum Collections, Casper, Wyoming *2*, 1–33.

66. Carrano, M.T., Benson, R.B.J., and Sampson, S.D. (2012). The phylogeny of Tetanurae (Dinosauria: Theropoda). J. Syst. Palaeontology *10*, 211–300.
67. Birch, S.H., and Carrano, M.T. (2012). An articulated pectoral girdle and forelimb of the abelisaurid theropod *Majungasaurus crenatissimis* from the Late Cretaceous of Madagascar. J. Vertebr. Paleontol. *32*, 1–16.
68. Carrano, M.T. (2007). The appendicular skeleton of *Majungasaurus crenatissimus* (Theropoda, Abelisauridae) from the late Cretaceous of Madagascar. Society of Vertebrate Paleontology Memoir *8*, 163–170.
69. Novas, F.E. (1993). New information on the systematics and postcranial skeleton of *Herrerasaurus ischigualastensis* (Theropoda: Herrerasauridae) from the Ischigualasto Formation (Upper Triassic) of Argentina. J. Vertebr. Paleontol. *13*, 400–423.
70. Colbert, E.H. (1989). The Triassic dinosaur *Coelophysis*. Mus. North. Ariz. Bull. *57*, 1–160.
71. Raath, M.A. (1969). A new coelurosaurian dinosaur from the Forest Sandstone of Rhodesia. Arnoldia (Rhodesia) *4*, 1–25.
72. Osmólska, H., and Roniewicz, E. (1970). Deinocheiridae, a few family of theropod dinosaurs. Acta Palaeontol. Pol. *21*, 5–19.
73. Osmólska, H., Roniewica, H., and Barsbold, R. (1972). A new dinosaur, *Gallimimus bullatus* n. gen., n. sp. (Ornithomimidae) from the Upper Cretaceous of Mongolia. Palaeontologia Polonica *27*, 103–143.
74. Russell, D.A. (1972). Ostrich dinosaurs from the Late Cretaceous of western Canada. Can. J. Earth Sci. *9*, 375–402.
75. Jin, L., Chen, J., and Godefroit, P. (2012). A new basal ornithomimosaur (Dinosauria: Theropoda) from the Early Cretaceous Yixian Formation, Northeast China. In Bernissart Dinosaurs and Early Cretaceous Terrestrial Ecosystems, P. Godefroit, ed. (Indiana University Press), pp. 467–487.
76. Middleton, K.M., and Gatesy, S.M. (2000). Theropod forelimb design and evolution. Zool. J. Linn. Soc. *128*, 149–187.
77. Grafen, A. (1989). The phylogenetic regression. Philos. Trans. R. Soc. Lond. B Biol. Sci. *326*, 119–157.
78. Pinheiro, J., Bates, D., DebRoy, S., Sarkar, D., and Team, R.C. (2014). nlme: linear and nonlinear mixed effects models. R package version *3*, 1–117. https://CRAN.R-project.org/package=nlme.
79. Paradis, E., Claude, J., and Strimmer, K. (2004). APE: analyses of phylogenetics and evolution in R language. Bioinformatics *20*, 289–290.
80. R Core Team. (2017). R: a language and environment for statistical computing (R Foundation for Statistical Computing). https://www.r-project.org.
81. Felsenstein, J. (1985). Phylogenies and the comparative method. Am. Nat. *125*, 1–15.
82. Garland, T., Jr., and Ives, A.R. (2000). Using the past to predict the present: confidence intervals for regression equations in phylogenetic comparative methods. Am. Nat. *155*, 346–364.
83. Pagel, M. (1999). Inferring the historical patterns of biological evolution. Nature *401*, 877–884.
84. O'Leary, M.A., and Kaufman, S.G. (2012). MorphoBank 3.0: web application for morphological phylogenetics and taxonomy. https://www.morphobank.org.

STAR★METHODS

KEY RESOURCES TABLE

REAGENT or RESOURCE	SOURCE	IDENTIFIER
Biological Samples		
Xiyunykus pengi holotype	This paper	IVPP V22783
Bannykus wulatensis holotype	This paper	IVPP V25026
Deposited Data		
Character list for cladistic analysis	This paper	Data S1
Character/taxon matrix for cladistic analysis	https://morphobank.org/permalink/?P2127	Data S1
Forelimb length/body mass data	compiled from [41] and [42]	Data S1
Software and Algorithms		
Mesquite V 3.03	http://www.mesquiteproject.org/	N/A
TNT software	https://cladistics.org/tnt/	N/A
R software	https://www.r-project.org/	N/A
RASP (Reconstruct Ancestral State in Phylogenies)	http://mnh.scu.edu.cn/soft/blog/RASP/	N/A

CONTACT FOR REAGENT AND RESOURCE SHARING

Further information and requests for resources and reagents should be directed to and will be fulfilled by the Lead Contact, Xing Xu (xu.xing@ivpp.ac.cn).

EXPERIMENTAL MODEL AND SUBJECT DETAILS

The experimental subject is the fossilized holotypes of the alvarezsaurian dinosaurs *Xiyunykus pengi* (IVPP V22783) and *Bannykus wulatensis* (IVPP V25026), which are housed at the Institute of Vertebrate Paleontology and Paleoanthropology, Beijing, China. The sex states of both specimens are unknown, and both specimens are inferred to be at the sub-adult ontogenetic stage.

METHOD DETAILS

CT images

IVPP V22783 and IVPP V25026 were scanned using both 225kv (for small skeletal elements) and 450 kV (for large skeletal elements) micro-computerized-tomography apparatus (developed by the Institute of High Energy Physics, Chinese Academy of Sciences (CAS)) at the Key Laboratory of Vertebrate Evolution and Human Origins, CAS. A total of 720 transmission images were reconstituted into a stack of 1563 slices each measuring 2048*2048 pixels for each small-sized skeletal element, and a total of 1,440 transmission images were reconstituted into a stack of 2,048 slices each measuring 2048*2048 for each large-sized skeletal element, using two-dimensional reconstruction software developed by the Institute of High Energy Physics, CAS. 3D segmentation of the CT data was performed using Mimics (Version 10.01).

Histology

Histological thin sections of long bones were made using standard techniques. To minimize damage to the specimens, the fibulae of IVPP V22783 and IVPP V25026 were each dismantled at a natural break and then sectioned 5 mm from the preserved distal end of the proximal segment to ensure a nearly complete cross section. The proximal end of the distal segment was then re-attached to the proximal segment. Subsequently, both samples were embedded in resin, and diaphyseal transverse thin-sections were cut using a diamond circular saw fitted with a diamond-tipped wafering blade. One surface of each section was smoothed with a wheel grinder/polisher, and then ground manually using grinding powder (600 grit) to produce a smooth texture ideal for gluing to a glass slide. The section was then cut to a thickness of about 250 μm with a diamond circular saw before being ground further to the desired final thickness of 50–80 μm, leaving the exposed surface of the section smooth. Each slide was then cleaned in a water-filled ultrasonic cleaner to remove microscopic grit, and finally capped with a glass coverslip. The completed thin sections were studied in normal and polarized light.

Phylogenetic analysis

The data matrix was assembled in Mesquite v 3.03 [43], and comprises 113 species-level theropod taxa and 594 morphological characters (see below). Taxa were selected to broadly sample species from higher taxa within Maniraptora as well as from non-maniraptoran theropod outgroups, and were scored based on both primary observations of specimens and the literature. Character definitions were primarily based on previous work, largely by the authors, members of the Theropod Working Group [8, 9, 12, 20, 22, 33, 44–47], and alvarezsaur workers [1, 5, 12, 27, 32, 48, 49]. Twenty-three new characters were added to the dataset based on observations generated from this research (Data S1).

The matrix was subjected to phylogenetic analysis under the parsimony optimality criterion in TNT [50]. The search strategy employed alternating rounds of Sectorial Searches and Tree Drift [51] with default settings. The search for optimal topologies was terminated after stabilizing the consensus of most parsimonious topologies five times with a factor of 75. This strategy resulted in 144 most parsimonious trees (MPTs) of length 3202 steps, consistency index 0.218 and retention index 0.602. Further TBR swapping and Tree Drifting of the MPTs revealed additional, non-identical most-parsimonious topologies, but did not improve the length nor result in decreased resolution of the strict consensus relative to the initial 144 MPTs.

Strict consensus topologies (Figure S1) were calculated in TNT [50, 52] using this pool of 144 MPTs. Absolute Bremer support [53, 54] for nodes in the strict consensus was calculated in TNT and used a pool of trees created by TBR swapping on the 144 MPTs recovered from the initial analysis, saving suboptimal trees by up to 10 steps, and saving 10,000 trees. An additional Bremer support analysis was conducted using an identical pool of trees, but excluding the alvarezsaurid taxon *Kol ghuva* [55] from support calculations (Figure S1). Synapomorphies common to all trees (see below) were explored using TNT [50, 52]. Tree diagrams were edited for clarity and produced for publication using InkScape [56].

Biogeographic inference

To reconstruct the biogeographic history of global alvarezsaurians, a statistical dispersal-vicariance analysis (SDVA) of Alvarezsauria was performed in the program RASP, where maximum parsimony was used as the standard criterion. This analysis was conducted with the maximum areas set to 3 and maximum reconstructions set to 100, under the ''Allow Reconstruction'' and ''Allow Extinction'' options. The phylogenetic framework used in the SDVA comes from the strict consensus tree produced by the traditional search with the TBR branch-swapping algorithm in the program TNT. Prior to the SDVA, the codes of the strict consensus with a file format of TREES were divided into data of 12 most parsimonious trees that denote no polytomies in topologies (Figure S2). Here, ranges of the potential ancestral area(s) for each internal node of Alvarezsauria are restricted to Asia (A), South America (B), North America (C), Asia–North America (AC) and South America–North America (BC). The direct land link between Asia and South America is considered unavailable during the Jurassic and Cretaceous, although a land link between the two continents would have occurred through North America during that period (see Dr Ronald C. Blakey's online database at https://deeptimemaps.com).

Analysis of forelimb allometry and reduction

Dataset

We analyzed patterns of forelimb evolution using an extended version of the dataset of ref. [57], combined with mass estimates from ref. [58]. These mass estimates were based on the scaling relationship of femoral robustness presented by Campione et al. [19], an approach that has been shown to be relatively independent of phylogeny and limb orientation in extant tetrapods [59]. As such, it should provide a reasonable index of body size that is independent of body proportions. Many previous studies instead used length measurements, predominantly femoral length, as proxies for dinosaur body size (e.g., refs. [60–62]; and trunk length [63]). The use of femoral length is particularly problematic for studies of limb evolution, in which it would be difficult to distinguish changes in relative hindlimb length, or hindlimb proportions from proportional changes in just forelimb length (also discussed in ref. [63]).

Most of our sets of measurements came from single individuals, with two exceptions. First, measurements from two similarly-sized individuals of *Torvosaurus tanneri* were compiled to form a composite of the two specimens, using forelimb measurements from ref. [64] and body mass based on the femur of a specimen reported by Siegwarth et al. [65]; see Carrano et al. [66] for referral of these specimens to a single species). Second, forelimb measurements from one specimen of *Majungasaurus* [67] were combined with a body mass estimate for a similar-sized individual (FMNH PR 2278; ref. [68]). These steps were considered to be important because otherwise we would not have complete data from any member of Megalosauridae or Abelisauridae, clades with large body size and proportionally reduced forelimbs.

Total forelimb length was based on the summed lengths of the humerus, radius (sometimes an estimate based on measurement of the equivalent portion of the ulna), and longest digit. The longest digit is typically digit II in non-tetanuran theropods, and is digit III in most tetanurans (following the digital homologies used here, presented by ref. [24]; note that our digit III of tetanurans has been considered as homologous to digit II of non-tetanurans by many earlier studies). This is subject to some variation, as described below. Digit lengths were calculated excluding the ungual phalanx for two reasons. First, the ungual phalanx was frequently disarticulated and not preserved. Second, methods of reporting ungual lengths vary among publications. Some descriptions report proximodistal lengths along curved surfaces of the phalanx, whereas others report straight-line distances.

In total, N = 26 non-paravian theropod species in our dataset preserve sufficiently complete hand skeletons that the lengths of digits II and III (in non-tetanurans) or III and IV (in tetanurans) can be compared (including metacarpals and excluding ungual phalanges). Digit II (non-tetanurans) or III (tetanurans) is the longest digit in most of these species (N = 19), a condition that seems to be widespread across theropod phylogeny. Nevertheless, digit IV is longest in early theropods, and this condition is likely primitive

for Theropoda (*Herrerasaurus* [69]; and coelophysoids: *Coelophysis bauri* and *Coelophysis rhodesiensis* [70, 71]). Digit IV is longest in some ornithomimosaurs [41, 42, 72–75]. Based on this information, we used metacarpal II and digit II for computing total arm length in most non-tetanuran theropods, and metacarpal III and digit III in most tetanurans (following the digit homologies of ref. [24]). We used digit II and metacarpal II for *Mononykus*, the only parvicursorine that was sufficiently complete to be included in our analyses. And we used digit III and metacarpal III for *Herrerasaurus* and coelophysoids, and digit IV and metacarpal IV for ornithomimosaurs.

In total, N = 28 non-paravian theropod species included in our phylogeny provided estimates of both body mass and complete forelimb length (summed humerus, radius, metacarpal and digit lengths). This is fewer than the N = 46 species that provide information on both body mass and partial forelimb length (summed humerus, radius and metacarpal lengths, omitting digit lengths). Partial forelimb length was also analyzed here, for comparison with previous studies of theropod forelimb evolution (e.g. [57, 63, 76]; but see [61] for an example using complete forelimb length).

Phylogenetic regression of forelimb length on body mass

We used phylogenetic generalized least-squares regression (pGLS [77]) to quantify the allometric relationship of forelimb length on body mass in non-paravian theropods (Figure S3 and Table S2). Data were $\log_{10}$-transformed prior to analysis, and non-paravians were analyzed because previous studies identified a change in this relationship among paravian theropods, associated with an evolutionary increase in forelimb length [61]. This approach was implemented using the packages nlme 3.1-131 [78] and ape 4.1 [79] in the R version 3.3.3 [80]. We used a version of the phylogenies presented by Benson et al. [58], resolving polytomies at random, then calibrating the tree to time by (1) randomly assigning numerical ages to taxa from a uniform distribution between their maximum and minimum possible ages of occurrence, and (2) extending zero-length branches by setting a minimum branch duration of 1 Ma. The phylogeny was further modified by the addition of the alvarezsauroids *Bannykus*, *Xiyunykus* and *Tugulusaurus* following the phylogenetic results obtained in the present work. Results are reported across a sample of 100 time-calibrated phylogenies.

The pGLS method uses the covariances expected among taxa given a phylogenetic tree to modify the assumptions of ordinary least-squares regression. Principally, and unlike in ordinary least-squares, observations of species in a phylogeny have varying levels of non-independence from each other due to phylogenetic relationships. When Brownian motion [81] is assumed, pGLS is mathematically analogous to ordinary least-squares regression of phylogenetic independent contrasts [82].This represents a model in which strong phylogenetic signal is present in a relationship of interest due to evolution along lineages, causing the intercept of the relationship between variables to drift at a constant, non-directional and stochastic rate on the phylogeny.

Estimation of the phylogenetic signal in the relationship between forelimb length and body mass was done using Pagel's λ [83]. This is a parameter that scales the strength of phylogenetic signal between the inferred phylogeny with its branch lengths ($\lambda = 1$; i.e., Brownian motion), and a star phylogeny in which all taxa effectively represent independent observations ($k = 0$; for ultrametric trees; equivalent to ordinary least-squares regression).

DATA AND SOFTWARE AVAILABILITY

The holotypes of the alvarezsaurian dinosaurs *Xiyunykus pengi* (IVPP V22783) and *Bannykus wulatensis* (IVPP V25026) are accessible to both professionals and the general public. The matrix for phylogenetic analysis is given in Data S1, and is also available on Morphobank [84] at the following link: https://morphobank.org/permalink/?P2127. Mesquite V 3.03 is available at http://www.mesquiteproject.org; TNT software is available at https://cladistics.org/tnt/; R software is available at https://www.r-project.org; RASP is available at http://mnh.scu.edu.cn/soft/blog/RASP/.

Nomenclature

This published work and the nomenclatural acts it contains have been registered in ZooBank, the proposed online registration system for the International Code of Zoological Nomenclature. The ZooBank life science identifiers can be resolved and the associated information viewed by appending the life science identifiers to the prefix http://zoobank.org/. The life science identifiers (LSID) for this publication are urn:lsid:zoobank.org:pub:E60C9E1C-AEFF-4589-8C5A-A32C664DFD5E.